AGU PUBLICATIONS

JGR

Journal of Geophysical Research: Biogeosciences

RESEARCH ARTICLE
10.1002/2015JG003165

**Key Points:**
- Ten years postfire, 85% of fire-killed necromass remain in the forest
- Ten years postfire, fire-killed trees emit 0.6 Mg C $ha^{-1}$ $yr^{-1}$
- While decomposition from fire-killed trees last decades, their contribution to NEP is small

**Correspondence to:**
J. L. Campbell,
john.campbell@oregonstate.edu

**Citation:**
Campbell, J. L., J. B. Fontaine, and D. C. Donato (2016), Carbon emissions from decomposition of fire-killed trees following a large wildfire in Oregon, United States, *J. Geophys. Res. Biogeosci.*, *121*, 718–730, doi:10.1002/2015JG003165.

Received 10 AUG 2015
Accepted 7 JAN 2016
Accepted article online 12 JAN 2016
Published online 3 MAR 2016



# Carbon emissions from decomposition of fire-killed trees following a large wildfire in Oregon, United States

**John L. Campbell[1], Joseph B. Fontaine[2], and Daniel C. Donato[3]**

[1]Department of Forest Ecosystems and Society, Oregon State University, Corvallis, Oregon, USA, [2]School of Veterinary and Life Sciences, Murdoch University, Perth, Washington, Australia, [3]Washington State Department of Natural Resources, Olympia, Washington, USA

**Abstract** A key uncertainty concerning the effect of wildfire on carbon dynamics is the rate at which fire-killed biomass (e.g., dead trees) decays and emits carbon to the atmosphere. We used a ground-based approach to compute decomposition of forest biomass killed, but not combusted, in the Biscuit Fire of 2002, an exceptionally large wildfire that burned over 200,000 ha of mixed conifer forest in southwestern Oregon, USA. A combination of federal inventory data and supplementary ground measurements afforded the estimation of fire-caused mortality and subsequent 10 year decomposition for several functionally distinct carbon pools at 180 independent locations in the burn area. Decomposition was highest for fire-killed leaves and fine roots and lowest for large-diameter wood. Decomposition rates varied somewhat among tree species and were only 35% lower for trees still standing than for trees fallen at the time of the fire. We estimate a total of 4.7 Tg C was killed but not combusted in the Biscuit Fire, 85% of which remains 10 years after. Biogenic carbon emissions from fire-killed necromass were estimated to be 1.0, 0.6, and 0.4 Mg C $ha^{-1}$ $yr^{-1}$ at 1, 10, and 50 years after the fire, respectively; compared to the one-time pyrogenic emission of nearly 17 Mg C $ha^{-1}$.

## 1. Introduction

Forest fires have long been recognized as an important component of the global carbon cycle. Among natural processes, combustion ranks second after metabolic respiration in mineralizing terrestrial biomass to the atmosphere, fire mortality ranks second after litter production in transferring live aggrading biomass to decomposing necromass, and the pyrolysis of biomass by forest fires feeds a global pool of black carbon which is largely isolated from the biological cycle [*Singh et al.*, 2012]. The role of forest fire in the carbon cycle is especially important in today's changing climate, not only because of its direct contribution to greenhouse gas emissions but also because a warming climate is expected to increase frequency and intensity of wildfires [*Flannigan et al.,* 2000, 2009*; Moritz et al.,* 2012], pushing the terrestrial biosphere toward a new equilibrium wherein less carbon resides in forest biomass and more resides in the atmosphere. Furthermore, because forest fire behavior is viewed by many as manageable, its control is regularly included as part of comprehensive climate change mitigation strategies [*Campbell et al.,* 2012; *Bradstock et al.,* 2012].

Characterizing and quantifying the effects of fire on the flux of carbon from forests into the atmosphere requires an understanding of both pyrogenic emissions due to immediate combustion and the prolonged biogenic emissions due to the decomposition (heterotrophic mineralization of carbon) by fire-killed necromass. A recent wealth of empirical studies aimed at quantifying combustion across a range of forest fires has allowed us to both constrain estimates of pyrogenic emissions and predict how this flux may change under alternate fire regimes (see reviews by *Sommers et al.* [2014] and *Urbanski* [2014]). By comparison, less attention had been paid to the protracted loss of terrestrial carbon to the atmosphere through the decomposition of fire-killed trees and how this flux is expected vary in relation to fire behavior or change under alternate fire regimes [*Harmon et al.,* 2011a, 2011b; *Ghimire et al.,* 2012].

Carbon emissions via the decomposition of fire-killed trees differ from pyrogenic emissions in several important ways. First, we expect that pyrogenic emissions to be lower in magnitude and less tightly coupled to fire behavior than subsequent carbon emissions via decomposition of fire-killed trees. Since combustion of aboveground biomass in forest fires is typically confined to dead surface fuels and live foliage, pyrogenic carbon emissions in any given fire tend not to exceed 15% of a forest's live and dead biomass [*Campbell et al.*, 2007; *Urbanski*, 2014]. Moreover, since the majority of surface fuels are consumed in nearly all fire conditions, while standing biomass experiences little combustion even in a crown fire, it is difficult for a

high-mortality fire to combust much more than twice the amount of carbon than does a low-mortality fire. By contrast, subsequent carbon emissions through decomposition of biomass killed in the fire but not consumed may range from none (e.g., low-severity fires when no trees are killed) to all of the prefire biomass (e.g., high-severity fires when all trees are killed). For this simple reason, cumulative carbon emissions through decomposition of fire-killed trees may exceed pyrogenic emissions and are more dependent on fire behavior than are pyrogenic emissions.

Emissions through decomposition of fire-killed biomass also differ from pyrogenic emissions in their influence on Net Ecosystem Production (NEP). While pyrogenic emissions necessarily contribute to net ecosystem carbon balance, the flux itself is concentrated in time. By contrast, the protracted decomposition of fire-killed trees can contribute to disequilibrium in stand-level NEP for decades [*Bond-Lamberty and Gower*, 2008; *Harmon et al.,* 2011a; *Ghimire et al.,* 2012]. Theoretically, fire-induced disequilibrium in NEP will balance out to zero over sufficiently long time frames or spatial extents (after all, no tree ever escapes death and mineralization, fire only aggregates this inevitable emission in time). However, like many natural disturbances, the majority of area subject to high-mortality forest fire is the result of relatively few, very large events [*Malamud et al.,* 1998; *Reed and McKelvey,* 2002]. As such, the extent required for spatial neutrality in NEP to emerge may easily exceed any meaningful geographic boundary, and the time frame required for neutrality in NEP to emerge may easily exceed the meaningful continuity of any fire regime. Consequently, assessing the effects fire on the carbon exchange between forests and the atmosphere demands not only a mechanistic understanding of combustion, mortality, and decomposition (which we largely have) but also the ability to quantify these processes with enough context specificity to accurately account for individual fire events.

In this study, we evaluate the current and future carbon emissions attributable to the decomposition of trees killed but not combusted in the 2002 Biscuit Fire. This exceptionally large wildfire burned over 200,000 ha of mixed-conifer forest in southwest Oregon. Due to its diversity of forest types, forest age-classes, and severity of fire effects, the Biscuit Fire has served as a valuable case study for evaluating the effects of wildfire on carbon dynamics, including the following: pyrogenic emissions [*Campbell et al.,* 2007], export of soil carbon through erosion [*Bormann et al.,* 2008], and charcoal formation [*Donato et al.,* 2009a; *Heckman et al.,* 2013]. In *Campbell et al.* [2007] we reported biomass combustion for 25 functionally distinct carbon pools. Then, using measures of prefire biomass and fire effects on 180 one hectare inventory plots, we estimated fire-wide pyrogenic emissions. In this current companion study, we report the 10 year decay status of various biomass pools killed, but not combusted, by the Biscuit Fire. Then, using measures of fire mortality on the same 180 inventory plots as before, we estimate current and future fire-wide emissions resulting from the decomposition of fire-killed trees. Our specific objectives are as follows:

1. Quantify mortality, dead tree fall rate, and decomposition rates specific to different species, parts (e.g., root, bole, and branch), physical setting, prefire stand history, and fire effects.
2. Using these stratified parameters, calculate the current cumulative flux of carbon from fire-killed trees into the atmosphere and model its attenuation into the future.
3. Evaluate the current and future carbon emissions from fire-killed trees in the context of commensurate forest regrowth and other regional carbon fluxes, including the pyrogenic emissions from the same fire.

## 2. Methods

### 2.1. Study Site

The Biscuit Fire burned at a mix of severities across 200,000 ha of forest in the Siskiyou Mountains of southwestern Oregon and northern California in the summer of 2002, making it the largest contiguous forest fire on record for Oregon (Figure 1). The Siskiyou Mountains are characterized by a wide variety of forest types, from Douglas fir/western hemlock/bigleaf maple communities on mesic sites, to Douglas fir/tanoak on drier sites, to Jeffrey pine on ultramafic substrates *Whittaker* [1960]. A general description of the Biscuit Fire and the forests it affected can be found in *Halofsky et al.* [2011].

### 2.2. Decomposition of Fire-Killed Trees

As illustrated in Figure 2, decomposition of fire-killed trees was computed as the collective mass loss to the atmosphere, over a specified period, from three primary pools representing different physical orientations:

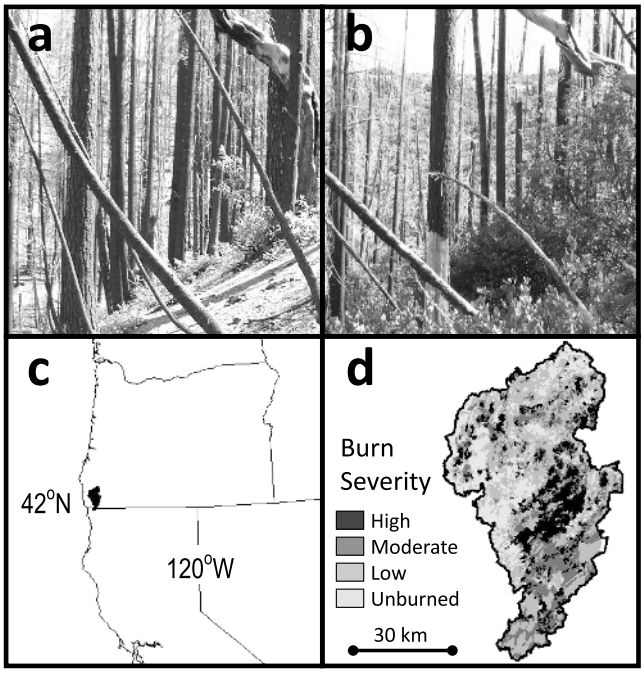


**Figure 1.** The 2002 Biscuit Fire showing (a) representative fire effects in 2004, (b) the same location in 2012, (c) location of the fire in the U.S. Pacific states of North America, and (d) remotely detected fire severity distribution. High = >90% overstory mortality, unburned = no overstory mortality but typically experiences surface fire.

standing necromass, fallen necromass, and buried necromass (i.e., dead root mass). Three separate rate constants defined mass loss to the atmosphere from standing, fallen, and buried necromass pools, respectively. Two additional rate constants defined transfer of mass from the standing to fallen pool by fragmentation and whole-tree fall, respectively. This three-pool, five-flux model was further stratified by tree part, namely, bole, branch, bark, and foliage (in the standing and fallen pools), and coarse root and fine root (in the buried pool). Boles were further stratified into three diameter classes, and all pools were stratified into three species groups (i.e., pines, non-pine conifers, and hardwoods) and three climatic zones (representing potentially different decomposition regimes) defined by aggregate plant association group and nominally corresponding to mesic, dry, and higher-elevation regions within the Biscuit Fire [*Donato et al.,* 2009b].

To estimate flux rates, we fit empirical observations of mass loss over time to a single-exponential model *Olsen* [1963] of the form:

$$M_t = M_0\left(e^{-kt}\right) \quad (1)$$

where $M_t$ is the mass of a specified necromass pool at time $t$, $M_0$ is the mass of the same pool immediately following its death by fire and any assessed combustion, and $t$ is the elapsed time since the fire (~10 years in this study). In this way, the rate constant $k$ not only describes the cumulative mass loss at year $t$ but can also be used to extrapolate mass loss into the future. The accuracy of such extrapolation does, however, depend on the assumption that loss rates remain constant over time, which may be violated if either the environment in which decay is occurring changes or if discriminating decay renders mixed substrates more recalcitrant over time. Extrapolation of our decay model does not account for climate-driven changes in the decay environment, but our model does account for important changes in decay that occur after wood

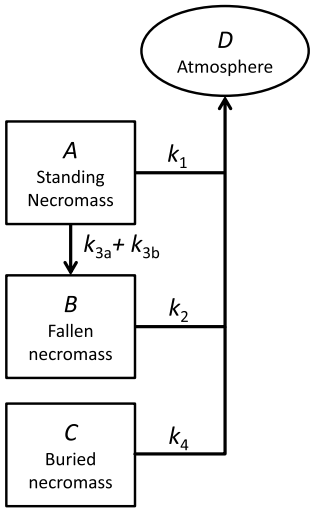


**Figure 2.** Approach to computing biogenic decomposition of fire-killed necromass. Decomposition was calculated separately for each plant tissue class according to five first-order exponential rate constants. The constant $k_1$ is the decomposition of necromass in its standing state; $k_2$ is the decomposition of necromass in its fallen state; $k_{3a}$ and $k_{3b}$ are the transfers between standing and fallen states, via whole-tree fall and fragmentation, respectively; and $k_4$ is the decomposition of buried roots.

**Table 1.** Methodology and Sampling Design for Determination of Rate Constants[a]

| | |
|---|---|
| *Aerial Decay: $k_1 = ln(D_0/D_t)/t$, where $D_0$ = live tree part density, $D_t$ = density of standing fire-killed tree part circa 2012, and t = elapsed time since fire* | |
| Bole | $D_t$ measured for 198 trees, stratified by species group (Douglas fir, pine species, and pacific madrone), diameter class (range 7 to 146 cm DBH), and climatic zone (defined by aggregate plant association group, nominally corresponding to mesic, dry, and higher-elevation regions within the Biscuit fire). Tree-average density was calculated as the average density of three transverse samples (cookies) collected from the lower, middle, and upper third of each tree, weighted by a factor of 0.60, 0.36, and 0.04, respectively, to account for volume proportion by height (derived from the taper equations of *Arney* [2009]). $D_0$ assumed to be 0.39, 0.45, and 0.58 g $cm^{-3}$ for sugar pine, Douglas fir, and pacific madrone, according to *Maeglin and Wahlgren* [1972], *USFS* [1965], and Wood Data Base, respectively. |
| Branch | $D_t$ measured for 259 branches stratified by diameter (range 1 to 56 mm) collected from the 198 standing dead trees described above. $D_0$ measured for 55, similarly stratified live tree branches samples. |
| Bark | Bark density loss was not directly measured in this study. Based on *Allison and Murphy* [1963], we crudely assumed bark to decompose at one half the rate of bole wood of the same species. Anecdotally, bark from fire-killed trees in this study regularly showed evidence of charring and fragmentation but not any apparent density loss. |
| Foliage | Aerial decay rates of fire-killed foliage are computationally inconsequential, not only because fire mortality on the Biscuit most often entailed full foliage combustion [*Campbell et al.,* 2007] but also because fall rates of fire-killed foliage approach totality within the first year after mortality such that nearly all decay occurs on the ground. As such, foliage aerial decay rates were arbitrarily set to 0.5 $year^{-1}$. |
| *Surface Decay: $k_2 = ln(D_0/D_t)/t$, where $D_0$ = live tree part density, $D_t$ = density of fire-killed tree part having fallen to ground shortly after fire, and t = elapsed time since fire* | |
| Bole | $D_t$ measured on 60 fallen logs, deduced to have been killed in the Biscuit Fire (by presence of surface charring) and fell within the next year (saw cuts datable to known salvage operations); stratified by species group (see above), diameter class (range 7 to 146 cm DBH), and climatic zone (see above). Density was determined from a single transverse sample (cookie) taken from the center of each log. $D_0$ as described above for areal bole decay. |
| Branch | $D_t$ measured for 86 branch samples, stratified by diameter (range 1 to 72 mm) collected from the 60 fallen logs described above. $D_0$ as described above for areal branch decay |
| Bark | Crudely assumed to be one half the rate of fallen bole wood (see above for aerial bark decay). |
| Foliage | Given the short residence times of leaf litter (relative to wood and bark), and the exceptionally small portion of fire-filled biomass represented by uncombusted foliage [*Campbell et al.,* 2007], we chose to avoid the hazard of false accuracy and simply assign foliage decomposition rates the arbitrarily rapid rate of 0.5 $year^{-1}$. |
| *Whole-tree Fall Rate: $k_{3a} = ln(C_0/C_t)/t$, where $C_0$ = count of standing dead trees circa 2004, $C_t$ = count of standing dead trees ca 2013, and t = elapsed time between samples* | |
| Whole tree | Before-and-after stem surveys conducted at 44 independent and dispersed study plots, including a total sample size of >3000 fire-killed trees ranging in size from 2 to 198 cm DBH. |
| *Fragmented Fall Rate: $k_{3b} = ln(M_0/M_t)/t$, where $M_0$ = mass of standing tree parts circa 2004, $M_t$ = mass of standing tree parts circa 2012, and t = elapsed time between samples* | |
| Bole | $M_0$ allometrically modeled from DBH with the assumption that each tree was live and entire. $M_t$ is the same value, corrected to account height loss due to observed breakage. Assessed for each of the 3000 fire-killed trees described above. |
| Branch | $M_0$ allometrically modeled from DBH with the assumption that each tree was live and entire. Each fire-killed tree surveyed in 2014 was binned into one of four fragmentation classes through ocular assessment, corresponding to an $M_t$ of 0.05 $M_0$, 0.15 $M_0$, 0.60 $M_0$, and 1.0 $M_0$, respectively. |
| Bark | $M_0$ allometrically modeled from DBH with the assumption that each tree was entire. Each fire-killed tree surveyed in 2014 was binned into one of four fragmentation classes through ocular assessment, corresponding to an $M_t$ of 0.0, 0.25 $M_0$, 0.75 $M_0$, and 1.0 $M_0$, respectively. |
| Foliage | Practically all uncombusted foliage retained on fire-killed trees fell to the ground within the first year after the fire. To account for this in our decomposition model (constructed only of first-order exponential rate constants) we set the rate constant describing dead foliage fall to 5.0 $year^{-1}$. |
| *Buried Decay: $k_4$ = first-order exponential decay constants according to named authors* | |
| Coarse root | $k = 0.02$ $year^{-1}$ according to *Janisch et al.* [2005] assessment of Douglas fir roots > 1.0 cm diameter. |
| fine root | $k = 0.20$ $year^{-1}$ according to *Chen et al.* [2002] and *Fogel and Hunt* [1979] for various tree roots < 1.0 cm diameter. |

[a]Dead wood density was determined after oven drying at 95°C to constant mass; an 8% downward correction was then applied to account for oven shrinkage and afford direct comparison with published green tree densities [*Glass and Zelinka*, 2010].

transitions from the aerial to surface environment. Furthermore, by disaggregating our necromass pools (i.e., into bole, branch, bark, foliage, root, species group, and size class) our model minimizes the changes in recalcitrance that any one pool may experience over time [*Freschet*, 2012]. The specific sampling methods used to determine $M_t$ and $M_0$ for each necromass category are detailed in Table 1. Note that while the form of equation (1) was used in computing all flux rates, at times, density, volume, or count was operationally substituted for mass.

### 2.3. Initial Fire-Killed Biomass

Within the perimeter of the Biscuit Fire there are 180 regularly spaced permanent federal inventory plots, all of which received postfire measurements in 2003 or 2004 [*Azuma et al.,* 2004]. It is well established that injury caused by fire can sometimes contribute to tree death several years after being burned [*Filip et al.,* 2007].

Our assessment operationally defines fire mortality as trees which died within 1–2 years after the fire. Any subsequent mortality and ensuing decomposition, though perhaps related to fire, was not in this study directly attributed to the Biscuit Fire.

For each tree identified in the inventory plots as having been killed in the Biscuit Fire, we estimated the mass of its fine roots, coarse roots, bole, branch, bark, and foliage as if it were alive and whole. From each of these parts, we then subtracted the proportion estimated to have been combusted in the fire according to *Campbell et al.* [2007] to yield a tree-specific $M_0$ for each of its component parts. Bole mass was estimated using species- and site-specific allometric equations relating stem diameter to volume and species-specific wood density values [*van Tuyl et al.,* 2005]; foliage and bark mass were estimated directly from species- and site-specific allometric equations [*Means et al.,* 1994]; coarse root mass was assumed to be 0.31 times the bole mass (an average of regionally representative, plot-level ratios, allometrically estimated by *Campbell et al.* [2004a]); and fine root mass was assumed to be 0.16 times the bole mass (an average of regionally representative, plot-level ratios directly sampled by *Campbell et al.* [2004b]). Total biomass was converted to carbon mass assuming a carbon concentration of 0.5 for all woody parts and 0.45 for foliage. These tree-level values for $M_0$ were then summed across each inventory plot as to be expressed in carbon mass per unit ground area.

### 2.4. Fire Severity and Scaling Across the Fire

For evaluating the direct effects of fire severity on subsequent carbon emissions, fire severity was calculated, for each of the 180 inventory plots, as the fraction of initial live basal area (including all woody stems $>=2.5$ cm diameter breast high (DBH)) killed in the Biscuit Fire. For the purpose of scaling plot-level measurements to the entire Biscuit Fire it was necessary to use a mapped assessment of fire severity. Specifically, plot-level estimates of decomposition were scaled-up to the entire Biscuit Fire according to mapped fire severity classification and whether or not a site had burned in the Silver Fire (a major fire which burned 13 years prior to the Biscuit Fire). Such strata accounted only for variation in $M_0$ (tree mass killed in the Biscuit Fire), as the rate constants $k$ were assumed to be the same among plots. We employed the same BAER (Burned Area Emergency Response) severity classification map used earlier by *Campbell et al.* [2007]. Since this time, improved maps of Biscuit Fire severity have been built [*Thompson and Spies,* 2009], but we felt it was more important to maintain consistency between our pyrogenic and biogenic accounting. Moreover, since the 180 inventory plots are distributed widely in space and randomly with respect to actual fire effects, misclassification by BAER, or any other severity map, does not bias fire-wide estimates of carbon flux.

### 2.5. Uncertainty Propagation

For this study, we assumed the inventory-based estimates of fire-killed necromass to be largely accurate and limited our uncertainty analysis to that associated with decomposition rates. To account for this uncertainty, we computed alternate estimates of total carbon emissions using an upper and lower values for the rate constants defining mass loss to the atmosphere. Uncertainty in mass loss from standing and fallen necromass pools ($k_1$ and $k_2$ in Figure 2) were based on the upper and lower 95% confidence intervals in dead wood density (among samples collected in 10 years after death). Since we relied on crude literature values for root decay, uncertainty in mass loss from buried necromass pools ($k_4$ in Figure 2) was generously set to plus and minus 20% density loss at 10 years after death.

## 3. Results

### 3.1. Fire Mortality

Prefire live aboveground and belowground biomass among the 180 inventory plots ranged from 1 to 502 (median = 161) Mg C ha$^{-1}$ depending somewhat on site quality but largely disturbance history (i.e., whether sites had experienced late twentieth century fire). Fractional tree mortality, which was largely independent of prefire biomass, ranged from zero to totality. As a result the necromass killed but not combusted among the 180 inventory plots ranged from 0 to 352 (median = 24) Mg C ha$^{-1}$ . Despite smaller trees being more abundant, more often killed, and only somewhat more combusted than larger trees, fire mortality in the form of large-diameter (>30 cm DBH) boles and their associate coarse roots made up greater than 40% of all other fire-killed biomass combined. The remaining uncombusted fire mortality is composed of smaller diameter wood, bark, fine roots, and foliage in that order (Table 2). Overall the Biscuit Fire killed and left uncombusted a total of 10.4 Tg C (an average of 51 Mg C ha$^{-1}$).

**Table 2.** Biomass Killed But Not Combusted in Biscuit Fire (kg C ha$^{-1}$)

| | Biscuit Fire Severity[a] | | | | | | | |
|---|---|---|---|---|---|---|---|---|
| | Not Burned 15 years Earlier in Silver Fire | | | | Also Burned 15 years Earlier in Silver Fire | | | |
| Necromass Pool | High | Moderate | Low | Unburned Very Low | High | Moderate | Low | Unburned Very Low |
| | | | | *Foliage* | | | | |
| Small conifers | 19 | 62 | 58 | 26 | 0 | 0 | 4 | 2 |
| Small hardwoods | 31 | 23 | 57 | 99 | 2 | 42 | 29 | 67 |
| Medium conifers | 135 | 367 | 232 | 131 | 0 | 1 | 32 | 29 |
| Medium hardwoods | 292 | 77 | 354 | 606 | 3 | 151 | 289 | 763 |
| Large conifers | 180 | 384 | 409 | 162 | 0 | 242 | 67 | 190 |
| Large hardwoods | 52 | 7 | 67 | 162 | 0 | 37 | 98 | 46 |
| | | | | *Branch* | | | | |
| Small conifers | 130 | 115 | 88 | 34 | 0 | 13 | 6 | 3 |
| Small hardwoods | 144 | 37 | 106 | 159 | 146 | 142 | 50 | 120 |
| Medium conifers | 1207 | 981 | 501 | 247 | 0 | 83 | 78 | 60 |
| Medium hardwoods | 1778 | 183 | 1026 | 1407 | 53 | 1130 | 806 | 2202 |
| Large conifers | 3279 | 1837 | 1438 | 523 | 0 | 2598 | 350 | 683 |
| Large hardwoods | 835 | 23 | 280 | 610 | 0 | 2540 | 387 | 211 |
| | | | | *Bark* | | | | |
| Small conifers | 111 | 109 | 86 | 34 | 0 | 12 | 6 | 3 |
| Small hardwoods | 76 | 22 | 65 | 100 | 75 | 83 | 31 | 76 |
| Medium conifers | 1284 | 1184 | 607 | 314 | 0 | 95 | 95 | 78 |
| Medium hardwoods | 1314 | 135 | 861 | 1207 | 44 | 955 | 701 | 1917 |
| Large conifers | 5019 | 3097 | 2641 | 962 | 0 | 4760 | 639 | 1281 |
| Large hardwoods | 877 | 23 | 318 | 748 | 0 | 2944 | 446 | 237 |
| | | | | *Bole* | | | | |
| Small conifers | 537 | 409 | 328 | 146 | 0 | 69 | 28 | 13 |
| Small hardwoods | 1220 | 250 | 876 | 1348 | 1333 | 1272 | 416 | 974 |
| Medium conifers | 7058 | 5254 | 2734 | 1425 | 0 | 555 | 462 | 401 |
| Medium hardwoods | 16733 | 1559 | 9027 | 12772 | 557 | 10730 | 7152 | 15988 |
| Large conifers | 31100 | 16967 | 13599 | 4950 | 0 | 28981 | 3632 | 6380 |
| Large hardwoods | 6885 | 186 | 2206 | 4947 | 0 | 21250 | 3576 | 1461 |
| | | | | *Roots* | | | | |
| Small conifers | 193 | 147 | 118 | 52 | 0 | 25 | 10 | 5 |
| Small hardwoods | 439 | 90 | 315 | 485 | 479 | 457 | 150 | 350 |
| Medium conifers | 2538 | 1890 | 983 | 512 | 0 | 199 | 166 | 144 |
| Medium hardwoods | 6017 | 561 | 3246 | 4593 | 200 | 3858 | 2572 | 5749 |
| Large conifers | 11184 | 6101 | 4890 | 1780 | 0 | 10422 | 1306 | 2294 |
| Large hardwoods | 2476 | 67 | 793 | 1779 | 0 | 7642 | 1286 | 525 |

[a]As determined by remotely sensed BAER severity classification. Values are the average of 24, 36, 42, and 34 inventory plots for high, moderate, low, and unburned very low severity plots not burned prior in the Silver fire, respectively; and the average of 1, 2, 14, and 5 inventory plots for high, moderate, low, and unburned very low severity plots burned prior in the Silver fire, respectively. Small trees are <10 cm DBH, medium trees are 10–20 cm DBH, and large trees are >20 cm DBH. For our decomposition calculations, conifers were further partitioned into pine and nonpine species (data not shown here), and roots were partitioned into coarse roots and fine roots, consistently computed as 0.66 and 0.34 total root mass, respectively.

### 3.2. Decomposition Rates

The measured densities of standing and fallen fire-killed wood, from which decomposition rates were calculated, are shown in Figure 3. An analysis of variance performed on the decomposition rates calculated for over 198 sampled tree boles revealed significant effects of species (with Douglas fir decomposing only slightly faster than pine species and pacific madrone) and condition (fallen logs decomposing only slightly faster than standing snags), but nonsignificant effects of geographic zone (mesic, dry, or high elevation) or size (diameter class). The single-exponent decomposition constants (fit to a single 10 year data point and used to subsequently model carbon emissions) are shown in Table 3.

### 3.3. Tree Fall Rates

As shown in Table 4, a greater fraction of fire-killed biomass fell from the canopy to the ground in 10 years through whole-tree fall than through fragmentation. The proportion of whole trees having fallen after

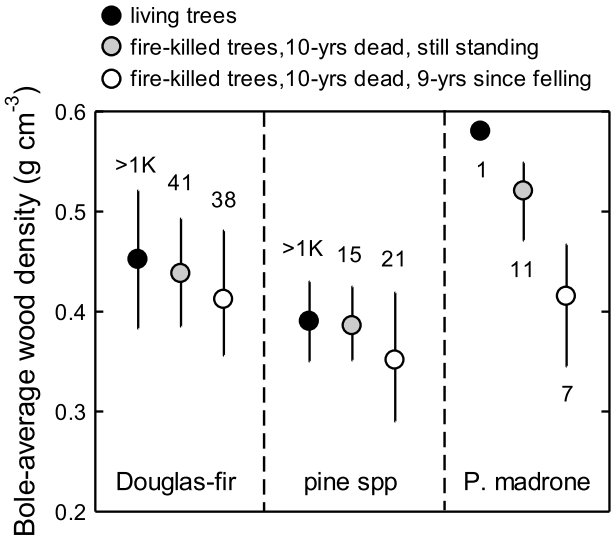


**Figure 3.** Wood density of green trees (live), fire-killed trees still standing 10 years after death (snags), and fire-killed trees 10 years after death and near immediate falling (logs). Sample size (shown near each symbol) is the number of independent trees sampled, with the density of each being determined as the taper-weighted average density of three cross-sectional subsamples taken along the length of each tree. Variability in wood density among trees is shown as the standard deviation (upper and lower error bars are the average positive and negative residuals of the mean, respectively; except for green trees where only a single symmetrical standard deviation was available from source literature, and green madrone where no variance was reported). Live wood densities are from *Maeglin and Wahlgren* [1972], *US Forest Service* [1965], and *Wood Data Base*, for pine species, Douglas fir, and Pacific madrone, respectively. Dead wood densities are those measured in the present study.

10 years was 20 times greater for smaller diameter trees (<20 cm DBH) than for larger diameter trees. Neither whole-tree fall rate nor fragmentation rate varied according to community type (used here as a proxy for decomposition regime). Across species, size class, and location, 57% of the trees killed in the Biscuit Fire are still standing 10 years after their death and have on average lost only 26% of their postcombustion necromass via fragmentation.

### 3.4. Biogenic Emissions

The amount of carbon released through the decomposition of fire-killed trees in the first 10 years following the Biscuit Fire is estimated to be 1.3 to 1.6 Tg C (or 6.5 to 7.8 Mg C $ha^{-1}$). As shown in Table 5, the largest contributing pools were those with the largest initial mass (i.e., bole wood and coarse root), not those with the highest decomposition rates (foliage and fine roots). Extrapolating our 10 year estimates of fall rates and decomposition rates back to the first year following fire and forward to 100 years after fire reveals several emergent patterns. Partitioning emission rates among necromass pools (Figure 4a) illustrates not only differential decay rates (responsible for the inflection point in collective emissions) but also an important 10 year lag in peak emissions from bole, branch, and bark, which results from a particular combination of aerial decay rates, fall rates, and surface decay rates. Total emissions from fire-killed necromass over time exhibit a distinct inflection point approximately five years following the fire (Figure 4b). Such inflection points are indicative of mixed substrate decay and in this case occur when the more labile foliage and fine root pools have become largely exhausted leaving the more recalcitrant wood and coarse roots. Overall, half of the Biscuit-killed necromass will still remain 50 years after the fire, at which time emissions from this single mortality cohort will be approximately 25 Mg C $ha^{-1}$ $yr^{-1}$ (Figure 4c).

The total amount of fire-killed necromass explained 99% of the variation in post fire decomposition among the 180 study plots (Figure 5a), indicating that variation in prefire species composition and tree size class was of

**Table 3.** Decomposition Constants for Fire-Killed Necromass[a]

| | Decomposition Constant $k$ ($year^{-1}$) | |
|---|---|---|
| Necromass Pool | Aerial Decay(Standing Snags) | Surface Decay(Fallen Logs and Debris) |
| | *Bole* | |
| Nonpine conifers | 0.010 (0.008–0.012) | 0.016 (0.013–0.019) |
| Pines | 0.001 (0.001–0.004) | 0.010 (0.005–0.014) |
| Hardwoods | 0.010 (0.008–0.012) | 0.016 (0.014–0.018) |
| | *Branch* | |
| All species | 0.014 (0.013–0.015) | 0.010 (0.008–0.012) |

[a]Decomposition constant $k = \ln(\text{Density}_{\text{live}}/\text{Density}_{11\text{ years dead}})/11$ years. Upper and lower estimates shown in parentheses were computed using standard error of the mean $\text{Density}_{11\text{ years dead}}$. See Table 1 for assumptions regarding decomposition of other fire-killed necromass pools such as foliage, bark, and roots.

**Table 4.** Fall Rate of Fire-Killed Necromass[a]

| Necromass Pool | Number of Trees Sampled | Fraction Fallen After 10 years | | Fall Rate $k$ (year$^{-1}$) | |
|---|---|---|---|---|---|
| | | Via Whole-Tree Fall | Via Fragmented Fall | Via Whole-Tree Fall | Via Fragmented Fall |
| | | *Bole* | | | |
| Conifers (small) | 156 | 0.86 | | 0.177 | |
| Conifers (medium) | 407 | 0.36 | | 0.041 | |
| Conifers (large) | 805 | 0.03 | | 0.003 | |
| Hardwoods (all sizes) | 229 | 0.03 | 0.35 | 0.003 | 0.043 |
| Nonpine conifers (all sizes) | 1075 | | 0.16 | | 0.017 |
| Pines (all sizes) | 137 | | 0.14 | | 0.016 |
| | | *Branch* | | | |
| Conifers (small) | 156 | 0.86 | | 0.177 | |
| Conifers (medium) | 407 | 0.36 | | 0.041 | |
| Conifers (large) | 805 | 0.03 | | 0.003 | |
| Hardwoods (all sizes) | 229 | 0.03 | 0.41 | 0.003 | 0.053 |
| Nonpine conifers (all sizes) | 1075 | | 0.42 | | 0.054 |
| Pines (all sizes) | 137 | | 0.50 | | 0.070 |
| | | *Bark* | | | |
| Conifers (small) | 156 | 0.86 | | 0.177 | |
| Conifers (medium) | 407 | 0.36 | | 0.041 | |
| Conifers (large) | 805 | 0.03 | | 0.003 | |
| Hardwoods (all sizes) | 229 | 0.03 | 0.51 | 0.003 | 0.070 |
| Nonpine conifers (all sizes) | 1075 | | 0.48 | | 0.065 |
| Pines (all sizes) | 137 | | 0.57 | | 0.085 |

[a]Fall rate $k = \ln(\text{standing necromass}_{2004}/\text{standing necromass}_{2014})/10$ years. Small trees are $<10$ cm DBH, medium trees are 10-20 cm DBH, and large trees are $>20$ cm DBH.

little importance in dictating postfire decomposition. Moreover, since low-biomass stands often experienced high-fractional mortality and high biomass often experienced low-fractional mortality, fire severity (as assessed by fractional basal area mortality) was, by itself, an imprecise predictor postfire carbon emissions (Figure 5b).

## 4. Discussion

### 4.1. Fire Mortality

The necromass generated in high-severity portions of the Biscuit Fire (about 103 Mg C ha$^{-1}$) corresponds well to the 130–200 Mg C ha$^{-1}$ biomass held in mature and old-growth forests of the Klamath ecoregion according to the regional assessment of *Hudiburg et al.* [2009]. Between the ages of 50 and 100, these particular forests are estimated to experience tree mortality rates of just over one-half percent annually [*Hudiburg et al.*, 2009]. As such, when mature forests burned at high severity in the Biscuit, somewhere between 100 and 200 years of future mortality was compressed into a single event. When individual fires of this size and severity occur in high biomass forests, like those of western Oregon, the generation of decomposing necromass is

**Table 5.** Biogenic Emissions From Fire-Killed Necromass by Carbon Pool and Burn Severity Class

| Necromass Pool | Carbon Released (kg C ha$^{-1}$ After 10 years) | | | | Fire-Wide Emmissions[b] (Tg C Across 202,642 ha, After 10 years) |
|---|---|---|---|---|---|
| | High Severity[a] | Moderate Severity[a] | Low Severity[a] | Unburned Very Low Severity[a] | |
| Foliage | 676 | 887 | 949 | 1163 | 0.19 |
| Branch | 850 | 365 | 307 | 324 | 0.08 |
| Bark | 405 | 219 | 173 | 168 | 0.04 |
| Bole | 5450 | 2125 | 2095 | 2362 | 0.54 |
| Roots | 6040 | 2385 | 2164 | 2277 | 0.58 |
| Total | 13421 | 5982 | 5683 | 6294 | 1.44 (1.31–1.59)[c] |

[a]As determined by remotely sensed BAER severity classification.
[b]Fire-wide emissions calculated by weighting the emissions from each burn class by the area of that burn class over the fire perimeter.
[c]Upper and lower estimates based on propagated uncertainty in woody decomposition rate constants.

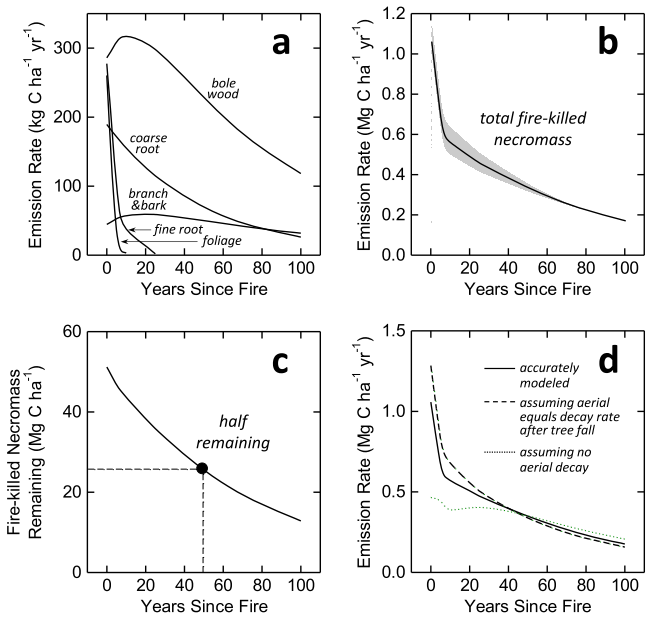


**Figure 4.** Temporal patterns of carbon emissions from fire-killed necromass, (a) partitioned by pool; (b) total, illustrating inflection point around year 5 and propagated uncertainty in decomposition rates (shaded band = 95% confidence interval); (c) approximate 50 year half-life; and (d) consequences of recognizing differential aerial and surface (fallen) decay rates.

notable at regional and even continental scales. The total amount of carbon transferred by the Biscuit Fire from aggrading living pools into decomposing dead pools was approximately three-quarters the average amount killed annually by wildfire throughout the entire western US (6 Tg C yr$^{-1}$) [*Hicke et al.,* 2013]. The distribution of fire mortality among different pools (Table 2) is a simple reflection of within-tree allometric proportions sans foliage which is commonly combusted in fire-killed trees. Understandably then, large-diameter wood made up the largest fire-generated necromass pool, more so in forests not recently burned where an even greater proportion of biomass was in the form of bole wood.

Due largely to the wide range of pre-fire biomass, fractional fire mortality (whether inferred through remote imagery, or direct ground measurement) was a poor predictor of absolute mortality and subsequent carbon emissions. While both intuitive and expected, this observation reminds us of the importance of accurately assessing preburn biomass in mapping and modeling fire effects on carbon dynamics.

### 4.2. Decay Rates

The wood density decomposition rates reported here fall comfortably within the range reported by other studies in the Pacific Northwest [*Sollins,* 1982; *Harmon et al.,* 1986; *Janisch et al.,* 2005; *Harmon et al.,* 2011b; *Dunn and Bailey,* 2012], which both validates our assessment and brings into question the need for additional field studies, at least those using single-exponent decay models fit to mass loss over a single time interval. In reality, necromass decay over time is expected to exhibit some initial lag (as substrates await decomposer colonization or fragmentation) and a decreasing proportional loss over time (as mixed substrates are reduced to their more recalcitrant fractions). By measuring mass loss across a chronosequence of dead wood, *Harmon et al.* [2000] demonstrated that dead wood decay can, in fact, exhibit such lags and tails in mass loss over time. Still, provided necromass pools are appropriately disaggregated (i.e., relatively recalcitrant and labile substrates assigned their own loss rate constants), single-exponent models like those used in this study fit empirical data just as well as multiparameter models [*Freschet,* 2012].

Given the recognized effects of moisture and temperature on decomposition, our inability to detect site effects on decomposition rate was likely a combination of measurement error (driven largely by our use of a single-species-specific green tree wood density in assessing mass loss for all wood fragments) and a wide variation in realized decay environments within the crude climate zones we recognized (Table 1). Given our samples were so widely distributed across our study area, our mean decomposition rates remain good estimates for our particular study. However, caution should be taken in applying these or any other landscape-average decomposition rates to any particular site, as decay rates of common substrates may vary across forest microenvironments by as much as 10 times, more so even than across large-scale climate gradients [*Vanderhoof*, 2013; *Bradford et al.,* 2014].

### 4.3. Fall Rates

The fall rates of standing necromass by fragmentation and whole-tree fall pertain to carbon emissions only to the degree that decomposition rates are different between the aerial and surface environments. It is commonly

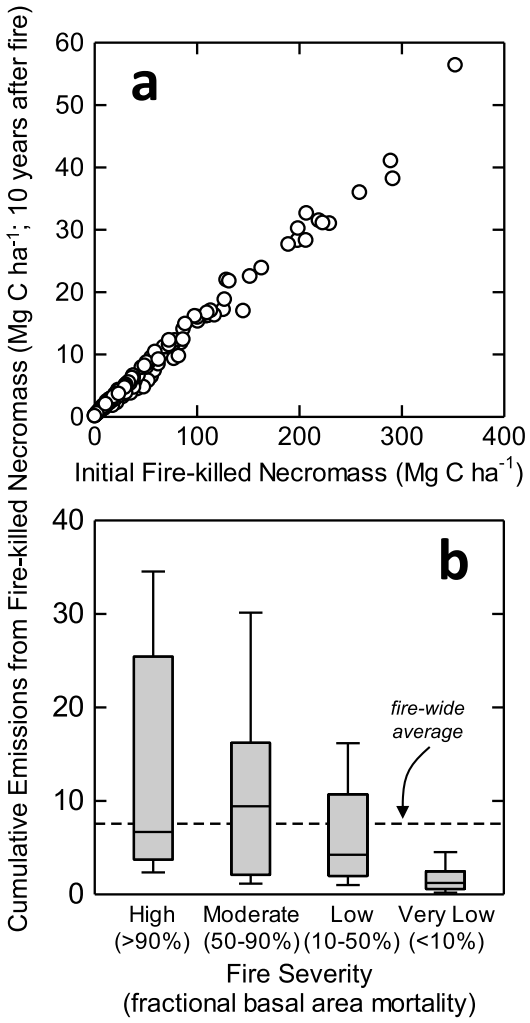


**Figure 5.** Carbon emissions from fire-killed necromass as a function of (a) absolute mortality and (b) fire severity among 180 inventory plots regularly stratified across the Biscuit Fire. Centerline, box, and whiskers, represent median, 25th percentiles, and range up to three-halves end quartiles (i.e., range excluding outliers), respectively. Fire severity (fractional tree basal area mortality) was directly determined for each plot (not remotely sensed).

assumed and consistently observed that decay rates of wood are slower in the drier aerial environment than in the moister surface environment [*Harmon et al.,* 2011b; *Yatskov et al.,* 2003; *Dunn and Bailey,* 2012]. Ecosystem models which apply the more commonly available surface decay rates to all fire mortality, without considering the decades many dead trees may spend in a standing condition, will inevitable overestimate initial emission rates and underestimate their duration. Similarly, models which assume negligible wood decay until a dead tree falls are prone to an inverse bias. The significance of tree fall rates in the timing of postfire carbon emissions is apparent in Figure 4a where peak emissions from branch, bark, and bole wood occur not immediately following the fire (when pool sizes are necessarily largest), but rather 10–20 years following the fire (after a requisite portion of the pool has fallen to the ground where it decays quicker). To further evaluate the relevance of tree fall on carbon emissions following the Biscuit Fire, we compared our fully parametrized model to others with alternate assumptions regarding fall rate and differential decay. As illustrated in Figure 4d, the largest bias occurred in the model which assumed wood remained undecayed until it fell to the ground. Applying a single surface decay rate to all wood did overestimate the near-term emission rates, but not as much as purported for other disturbed forests where both fall rates and the disparity between aerial and surface decay were determined to be higher than we observed in the Biscuit Fire [*Harmon et al.,* 2011b]. Moreover, once combined with the consistently attenuating emission from fire-killed roots and foliage, the fall-mediated lag in emissions from bole, branch, and bark did not produce a bimodal or "double-humped" emission pattern as it might have [*Harmon et al.,* 2011a].

Some authors have reported a brief (2 to 3 year) delay between tree mortality and the onset of measurable fall (see review by *Cluck and Smith* [2005]), suggesting that fall rates sometimes accelerate after passing some threshold in declining stability (e.g., root or basal decay). Since snag fall in this study is evaluated using stem attrition measured only at one-time point (10 years after death), we cannot resolve any early changes in fall rate. However, as a general rule, snag attrition measured over decades in prior studies conforms well to a first-order decay function as we have done here [*Everett,* 1999; *Cluck and Smith,* 2005]. Necromass decay over time is expected to exhibit some initial lag (as substrates await decomposer colonization or fragmentation) and a decreasing proportional loss over time (as mixed substrates are reduced to their more recalcitrant fractions).

### 4.4. Emission Rates

It is expected that dead wood dynamics operate over longer time scales in the Pacific Northwest than they do in other forests where environmental conditions or disturbance frequency prevent individual trees from growing as large. The analysis by *Spies and Franklin* [1988] suggests it would take >1000 years for woody

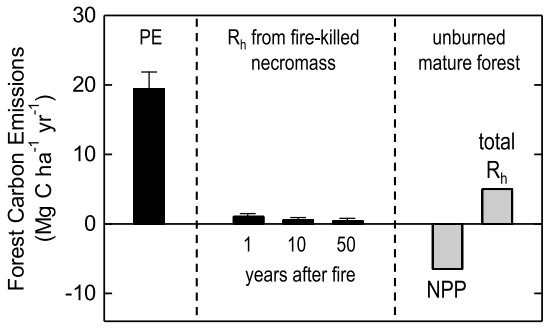


**Figure 6.** Forest carbon emissions from heterotrophic respiration ($R_h$) of necromass killed in the Biscuit fire, compared to the one-time pyrogenic emissions (PE) incurred during the fire and the biological fluxes typical of unburned mature forests of the Klamath region. Error bars on $R_h$ are propagated 95% confidence intervals in decomposition rates. Pyrogenic emissions and uncertainty estimated by *Campbell et al.* [2007]. Net Primary Production (NPP) modeled by *Turner et al.* [2007] and consistent with empirical observations of *Hudiburg et al.* [2009]. Total $R_h$, which includes both the heterotrophic fraction of soil surface efflux and dead wood decay, modeled by *Turner et al.* [2007] and consistent with empirical observations of *Campbell et al.* [2004a, 2004b].

debris to reach a site-level steady state in Western Oregon, and as such, most forests in the region exist in a state of dead wood disequilibrium defined by site-specific disturbance history. In this study, the measured magnitude and modeled duration of carbon released to the atmosphere through the decomposition of fire-killed trees speaks to how disturbance-generated mortality shapes not only the amount woody debris present at any given time, but in the exchange of carbon occurring between forest and atmosphere at any given time.

As shown in Figure 6, 10 years after the Biscuit Fire the annual flux of carbon from fire-killed trees into the atmosphere is estimated to be 0.6 Mg ha$^{-1}$ yr$^{-1}$, which is only 10% the total heterotrophic respiration rates to which these forests hypothetically equilibrate once mature [*Turner et al.,* 2007; *Campbell et al.,* 2004a] and only 3% the one-time pyrogenic emissions released during the fire [*Campbell et al.,* 2007]. Clearly, the capacity of this relatively modest carbon flux to shape carbon exchange between forest and atmosphere has not to do with its magnitude, but rather its duration and the fact that other ecosystem carbon fluxes such as net primary production, and potentially soil surface efflux, are greatly reduced in the initial period following wildfire.

Several studies suggest that high-severity wildfire, despite generating substantial additions to the dead wood pool, actually reduces total heterotrophic respiration by about one half [*Meigs et al.,* 2009; *Dore et al.,* 2012]. This is because wildfire typically consumes the forest floor (the substrate from which up to 30% of total heterotrophic respiration arises; *Campbell et al.* [2004b]) and temporally cuts off the supply of fine root turnover (a sizable contribution to belowground heterotrophic respiration). It was not the purpose of the paper to compute postfire NEP which would depend largely on uncertain patterns of forest regrowth and mineralization of soil carbon; however, NPP of regenerating and surviving vegetation need only reach 0.57 Mg ha$^{-1}$ yr$^{-1}$ by the 10 year following fire in order to compensate for the respiration from the remaining fire-killed necromass. Preliminary measurements (unpublished data) suggest that shrub production alone 10 years after the Biscuit Fire has already far exceeded this rate, consistent with other studies showing NPP over 1.5 Mg C ha$^{-1}$ by 2 years postfire in dry forests [*Irvine et al.,* 2007].

### 4.5. Regional Carbon Disequilibrium

Single, large disturbances like the Biscuit Fire make for valuable examples because they provide a broad range of conditions over which to stratify measurements. The specificity with which we evaluated mortality, fall, and decay within the Biscuit Fire was limited only by resources, not by opportunity. But quantifying the impacts of single events such as the Biscuit Fire also sheds light on the unique importance of rare events in shaping regional carbon exchange and the need to accurately account for them when either upscaling terrestrial measurements or downscaling atmospheric measurements.

It is reasonable to postulate, as *Odum* [1969], that over a sufficiently large landscape, disturbance-induced disequilibrium in any one location will be balanced in other locations experiencing similar disturbances at different times, and as long as the region-wide frequency of such disturbances remains constant, this shifting mosaic will operate with mass neutrality (e.g., NEP). However, within many ecoregions forest fires may not occur at fine-enough grain and high-enough frequencies for such equilibriums to arise. In fact, the self-organizing behavior of fire across landscapes dictates that most of the area burned in any given fire regime is the result of relatively few, very large events [*Malamud et al.,* 1998; *Reed and McKelvey,* 2002]. This disproportional impact of large infrequent disturbances thwarts landscape equilibriums in two dimensions. First, it can extend the area required to balance disturbance effects at any given time beyond meaningful ecological

boundaries. Second, it can extend the time horizon required for any bounded area to achieve equilibrium beyond the period we expect disturbance regimes to be reasonable stable. This second constraint on landscape equilibrium is especially relevant considering climate change may now be altering probabilistic fire regimes faster than the return interval of the most important events [*Zinck et al.,* 2011], rendering the realized impacts of fire on processes such as carbon emission wildly stochastic in space and time.

As illustrated in Figure 6, the carbon emissions attributed to the decomposition of trees killed in the Biscuit Fire documented in this study, as well as the pyrogenic emissions released by the Biscuit Fire documented in *Campbell et al.* [2007], attest to the importance single-disturbance events can have in regional carbon dynamics, especially in large biomass systems confined to relatively small ecological boundaries. Predicting the frequency of these rare events will be increasingly difficult in a changing environment, but our ability to accurately assess their impacts on regional carbon flux is slowly approaching sufficiency.

**Acknowledgments**

This work was supported, in part, by the Joint Fire Science Program, administered through the U.S. Bureau of Land Management in cooperation with the Department of Forest Ecosystems and Society at Oregon State University (project 11-1-1-4, cooperative agreement L11AC20276). The views and conclusions contained in this document are those of the authors and should not be interpreted as representing the opinions or policies of the U.S. Government or any other institution. We would like to extend special thanks to Melody Culp of the Rogue-Siskiyou National Forest for her invaluable assistance throughout the project. The data used in this study are available, without charge, by request of the corresponding author.

## References

Allison, F. E., and R. M. Murphy (1963), Comparative rates of decomposition in soil of wood and bark particles of several species of pines, *Proc. Soil Sci. Soc. Am.*, *27*, 309–312.

Arney, J. D. (2009), Tree taper profiles by species and region, Tree taper Article, For. Biom. Res. Inst., Corvallis, Oreg. [Available at http://www.arneyforest.com.]

Azuma, D. L., J. D. Donnegan, and D. Gedney (2004), Southwest Oregon Biscuit Fire: An analysis of forest resources and fire severity, *Res. Pap. PNW-RP-560*, U.S. Dep. of Agric., For. Serv., Pac. Northwest Res. Stn., Portland, Oreg.

Bond-Lamberty, B., and S. T. Gower (2008), Decomposition and fragmentation of coarse woody debris: Re-visiting a boreal black spruce chronosequence, *Ecosystems*, *11*(6), 831–840.

Bormann, B. T., P. S. Homann, R. L. Darbyshire, and B. A. Morrissette (2008), Intense forest wildfire sharply reduces mineral soil C and N: The first direct evidence, *Can. J. For. Res.*, *38*, 2771–2783.

Bradford, M. A., R. J. Warren, P. Baldrian, T. W. Crowther, D. S. Maynard, E. E. Oldfield, W. R. Wieder, S. A. Wood, and J. R. King (2014), Climate fails to predict wood decomposition at regional scales, *Nat. Clim. Change*, *4*, 625–630.

Bradstock, R. A., et al. (2012), Modelling the potential for prescribed burning to mitigate carbon emissions from wildfires in fire-prone forests of Australia, *Int. J. Wildland Fire*, *21*(6), 629–639.

Campbell, J. C., D. C. Donato, D. A. Azuma, and B. E. Law (2007), Pyrogenic carbon emission from a large wildfire in Oregon, USA, *J. Geophys. Res.*, *112*, G04014, doi:10.1029/2007JG000451.

Campbell, J. L., O. J. Sun, and B. E. Law (2004a), Disturbance and net ecosystem production across three climatically distinct landscapes, *Global Biogeochem. Cycles*, *18*, GB4017, doi:10.1029/2004GB002236.

Campbell, J. L., O. J. Sun, and B. E. Law (2004b), Supply-side controls on soil respiration among Oregon forests, *Global Change Biol.*, *10*, 1857–1869.

Campbell, J. L., M. E. Harmon, and S. R. Mitchell (2012), Can fuel reduction treatments really increase forest carbon sequestration by reducing future fire emissions?, *Front. Ecol. Environ.*, *10*(2), 83–90.

Chen, H., M. E. Harmon, J. Sexton, and B. Fasth (2002), Fine-root decomposition and N dynamics in coniferous forests of the Pacific Northwest, USA, *Can. J. For. Res.*, *32*, 320–331.

Cluck, D. R., and S. L. Smith (2007), Fall rates of snags: A summary of the literature for California conifer species, USDA, Forest Service Forest, Northeastern California Shared Service Area, Special Project Report: NE-SPR-07-01.

Donato, D. C., J. L. Campbell, J. B. Fontaine, and B. E. Law (2009a), Quantifying char in postfire woody detritus inventories, *Fire Ecol.*, *5*(2), 104–115.

Donato, D. C., J. B. Fontaine, J. L. Campbell, W. D. Robinson, J. B. Kauffan, and B. E. Law (2009b), Conifer regeneration in stand-replacement portions of a landscape-scale mixed-severity wildfire, *Can. J. For. Res.*, *39*, 823–838.

Dore, S., M. Montes-helu, S. C. Hart, B. A. Hungate, G. W. Kock, J. B. Moon, A. J. Frinkal, and T. E. Kolb (2012), Recovery of ponderosa pine ecosystem carbon and water fluxes from thinning and stand-replacing fire, *Global Change Biol.*, *18*, 3171–3185.

Dunn, C. J., and J. D. Bailey (2012), Temporal dynamics and decay of coarse wood in early seral habitats of dry-mixed conifer forests in Oregon's Eastern Cascades, *For. Ecol. Manage.*, *276*, 71–81.

Everett, R., J. Lehmkuhl, R. Schellhaas, and P. Ohlson (1999), Snag dynamics in a chronosequence of 26 wildfires on the East slope of the Cascade Range in Washington State, USA, *Int. J. Wildland Fire*, *9*(4), 223–234.

Filip, G. M., H. Maffei, and K. L. Chadwick (2007), Forest health decline in a central Oregon mixed conifer forest revisted after wildfire: A 25 year case study, *West. J. Appl. For.*, *22*(4), 278–284.

Flannigan, M. D., B. J. Stocks, and B. M. Wotton (2000), Climate change and forest fires, *Sci. Total Environ.*, *262*, 221–229.

Flannigan, M. D., M. A. Krawchuk, W. J. de Groot, B. M. Wotton, and L. M. Gowman (2009), Implications of changing climate for global wildland fire, *Int. J. Wildland Fire*, *18*, 483–507.

Fogel, R., and G. Hunt (1979), Fungal and arboreal biomass in a western Oregon Douglas-fir ecosystem: Distribution patterns and turnover, *Can. J. For. Res.*, *9*, 245–256.

Freschet, G. T., J. T. Weedon, R. Aerts, J. R. vanHal, and J. H. C. Cornelissen (2012), Interspecific differences in wood decay rates: Insights from a new short-term method to study long-term wood decomposition, *J. Ecol.*, *100*, 161–170.

Ghimire, B., C. A. Williams, G. J. Collatz, and M. Vanderhoof (2012), Fire-induced carbon emissions and regrowth uptake in western U.S. forests: Documenting variation across forest types, fire severity, and climate regions, *J. Geophys. Res.*, *117*, G03036, doi:10.1029/2011JG001935.

Glass, S. V., and S. L. Zelinka (2010), Moisture relations and physical properties, in *Wood Handbook, Wood as an Engineering Material*, *Gen. Tech. Rep. FPL-GTR-190*, 508 pp., U.S. Dep. of Agric., For. Serv., For. Prod. Lab, Madison, Wis.

Halofsky, J., *et al.* (2011), Mixed-severity fire regimes: Lessons from the Klamath-Siskiyou Ecoregion, *Ecosphere*, *2*(4), 40.

Harmon, M. E., et al. (1986), Ecology of coarse woody debris in temperate ecosystems, *Adv. Ecol. Res.*, *15*, 133–302.

Harmon, M. E., O. N. Krankina, and J. Sexton (2000), Decomposition vectors: A new approach to estimating woody detritus decomposition dynamics, *Can. J. For. Res.*, *30*, 76–84.

Harmon, M. E., B. Bond-Lamberty, J. Tang, and R. Vargas (2011a), Heterotrophic respiration in disturbed forests: A review with examples from North America, *J. Geophys. Res.*, *116*, G00K04, doi:10.1029/2010JG001495.

Harmon, M. E., C. W. Woodall, B. Fasth, J. Sexton, and M. Yatkov (2011b), Differences between standing and downed dead tree wood density reduction factors: A comparison across decay classes and tree species, *Res. Pap. NRS-15*, USDA For. Serv., North. Res. Stn.

Heckman, K., J. L. Campbell, H. Powers, B. E. Law, and C. Swanston (2013), The influence of fire on the radiocarbon signature and character of soil organic matter in the Siskiyou National Forest, Oregon, USA, *Fire Ecol.*, *9*(2), 40–56.

Hicke, J. A., J. H. Arjan, C. D. Allen, and C. A. Kolden (2013), Carbon stocks of trees killed by bark beetles and wildfire in the western United States, *Environ. Res. Lett.*, *8*, 1–8.

Hudiburg, T. M., B. E. Law, D. P. Turner, J. Campbell, D. Donato, and M. Duane (2009), Carbon dynamics of Oregon and Northern California forests and potential land-based carbon storage, *Ecol. Appl.*, *19*(1), 163–180.

Irvine, J., B. E. Law, and K. A. Hibbard (2007), Postfire carbon pools and fluxes in semiarid ponderosa pine in Central Oregon, *Global Change Biol.*, *13*, 1748–1760.

Janisch, J. E., M. E. Harmon, H. Chen, B. Fasth, and J. Sexton (2005), Decomposition of coarse woody debris originating by clearcutting of an old-growth conifer forest, *Ecoscience*, *12*(2), 151–160.

Maeglin, R. R., and H. E. Wahlgren (1972), Western wood density survey, *Rep. 2*, Res. Pap. FPL 183, USDA, For. Serv.

Malamud, B. D., G. Morein, and D. L. Turcotte (1998), Forest fires: An example of self-organized critical behavior, *Science*, *281*, 1840–1842.

Means, J. E., H. A. Hansen, G. J. Koerper, P. B. Alaback, and M. W. Klopsch (1994), Software for computing plant biomass: BIOPAK users guide, *Gen. Tech. Rep. PNW-GRT-340*, U.S. Dep. of Agric., For. Serv., Pac. Northwest Res. Stn., Portland, Oreg.

Meigs, G. W., B. E. Law, D. C. Donato, J. L. Campbell, and J. Martin (2009), Influence of mixed-severity wildfires on pyrogenic carbon transfers, postfire carbon balance, and regeneration trajectories in the eastern Cascades, Oregon, *Ecosystems*, *12*, 1246–1267.

Moritz, M. A., M. A. Parisienm, E. Batllori, M. A. Krawchuk, J. Van Dorn, D. J. Ganz, and K. Hayhoe (2012), Climate change and disruptions to global fire activity, *Ecosphere, 3*(6), 49.

Odum, E. P. (1969), The strategy of ecosystem development, *Science*, *164*, 262–270.

Olsen, J. S. (1963), Energy storage and the balance of producers and decomposers in ecological systems, *Ecology*, *44*, 322–331.

Pilip, G. M., C. L. Schmitt, D. W. Scott, and S. A. Fitzgerald (2007), Understanding and defining mortality in western conifer forests, *West. J. Appl. For.*, *22*(2), 105–115.

Reed, W. J., and K. S. McKelvey (2002), Power-law behaviour and parametric models for the size-distribution of forest fires, *Ecol. Modell.*, *150*, 239–254.

Sollins, P. (1982), Input and decay of coarse woody debris in coniferous stands in western Oregon and Washington, *Can. J. For. Res.*, *12*, 18–28.

Sommers, W. T., R. A. Loehman, and C. C. Hardy (2014), Wildland fire emissions, carbon, and climate: Science overview and knowledge needs, *For. Ecol. Manage.*, *317*, 1–8.

Spies, T. A., and J. F. Franklin (1988), Coarse woody debris in Douglas-fir forests of western Oregon and Washington, *Ecology*, *69*(6), 1689–1702.

Thompson, J. R., and T. A. Spies (2009), Vegetation and weather explain variation in crown damage within a large mixed-severity wildfire, *For. Ecol. Manage.*, *258*, 1684–1694.

Turner, P., D. Ritts, E. Law, B. Cohen, Z. Yang, T. Hudiburg, L. Campbell, and M. Duane (2007), Scaling net ecosystem production and net biome production over a heterogeneous region in the western United States, *Biogeosciences*, *4*(4), 597–612.

Urbanski, S. (2014), Wildland fire emissions, carbon, and climate: Emission factors, *For. Ecol. Manage.*, *317*, 51–60.

US Forest Service (1965), Western wood density survey, *Rep. 1*, Res. Pap. FPL 27, USDA, For. Serv.

Vanderhoof, M., C. Williams, M. Pasay, and B. Ghimire (2013), Controls on the rate of $CO_2$ emission from woody debris in clearcut and coniferous forest environments, *Biogeochemistry*, *114*, 299–311.

Van Tuyl, S., B. E. Law, D. P. Turner, and A. Gitelman (2005), Variability in net ecosystem production and carbon storage in biomass across forests: An assessment integrating data from forest inventories, intensive sites, and remote sensing, *For. Ecol. Manage.*, *209*, 273–291.

Whittaker, R. H. (1960), Vegetation of the Siskiyou Mountains, Oregon and California, *Ecol. Monogr.*, *30*, 279–338.

Yatskov, M., M. E. Harmon, and O. N. Krankina (2003), A chronosequence of wood decomposition in the boreal forests of Russia, *Can. J. For. Res.*, *33*, 1211–1226.

Zinck, R. D., M. Pascual, and V. Grimm (2011), Understanding shifts in wildfire regimes as emergent threshold phenomena, *Am. Nat.*, *178*(6), E149–E161.